Stereodynamic Properties of the Cooperative Homodimeric *Scapharca inaequivalvis* Hemoglobin Studied through Optical Absorption Spectroscopy and Ligand Rebinding Kinetics

Alberto Boffi,* Daniela Verzili,* Emilia Chiancone,* Maurizio Leone,‡ Antonio Cupane,‡ Valeria Militello,‡ Eugenio Vitrano,‡ Lorenzo Cordone,‡ Weiming Yu,§ and Ernesto E. Di Iorio§

*CNR Center of Molecular Biology, Department of Biochemical Sciences, University "La Sapienza" 00185 Roma, Italy; ‡Istituto di Fisica and GNSM—CISM, 90123 Palermo, Italy; and §Laboratorium fur Biochemie I, Eidgenössische Technische Hochschule, 8092 Zürich, Switzerland

ABSTRACT The study of the thermal evolution of the Soret band in heme proteins has proved to be a useful tool to understand their stereodynamic properties; moreover, it enables one to relate protein matrix fluctuations and functional behavior when carried out in combination with kinetic experiments on carbonmonoxide rebinding after flash photolysis. In this work, we report the thermal evolution of the Soret band of deoxy, carbonmonoxy, and nitric oxide derivatives of the cooperative homodimeric *Scapharca inaequivalvis* hemoglobin in the temperature range 10–300 K and the carbonmonoxide rebinding kinetics after flash photolysis in the temperature range 60–200 K. The two sets of results indicate that *Scapharca* hemoglobin has a very rigid protein structure compared with other hemeproteins. This feature is brought out i) by the absence of nonharmonic contributions to the soft modes coupled to the Soret band in the liganded derivatives, and ii) by the almost "in plane" position of the iron atom in the photoproduct obtained $\approx 10^{-8}$ s after dissociating the bound carbonmonoxide molecule at 15 K.

INTRODUCTION

The temperature dependence of the optical absorption spectra and of the ligand rebinding kinetics after flash photolysis provides information on different aspects of protein dynamics. In fact, the thermal behavior of the Soret band lineshape is influenced by the coupling of the electronic transition with high and low frequency vibrational modes as well as by homogeneous and inhomogeneous broadening (Srajer et al., 1986; Schomacker and Champion, 1986; Srajer and Champion, 1991). The various contributions to the overall bandwidth can be singled out by a suitable deconvolution of the band profile at various temperatures. Thereby, information on the stereodynamic properties of the active site and, in particular, on the presence of nonharmonic contributions to nuclear motions that play a relevant role in protein function can be obtained (Di Pace et al., 1992; Cupane et al., 1993a). On the other hand, analysis of the ligand rebinding kinetics after flash photolysis of the CO derivative enables one to establish a connection between protein matrix fluctuations and functional behavior (Steinbach et al., 1991; Di Iorio, 1992).

The unique structural and functional properties of the homodimeric component (HbI), contained in the red cells of the bivalve mollusc *S. inaequivalvis*, prompted the present study. In HbI cooperativity in ligand binding is based on direct transfer of information between the two heme groups that results from a unique assembly of the globin chains (Royer et al., 1989, 1990; Chiancone et al., 1990; Coletta et al., 1990). Thus, in HbI the heme-carrying E and F helices do not face solvent as in vertebrate hemoglobins, but form the subunit interface and thereby bring the heme groups into close contact (Fig. 1). Each heme group establishes a network of interactions with amino acid residues located in the F helix of the contralateral subunit within 1.5 helical turns of the proximal histidine. These interactions provide a direct link between the two heme groups and differ in detail in the liganded and unliganded forms of the protein. In HbI, therefore, the proximal histidine-Fe bond conduit does not play the same role as in vertebrate hemoglobins in communicating the state of ligation of one heme to the other subunit (Rousseau et al., 1993).

These distinctive characteristics of HbI stimulated the present study, in which optical spectroscopy and flash photolysis are used to investigate the dynamic properties of the protein and their functional relevance.

MATERIALS AND METHODS

HbI was extracted and purified according to the method of Chiancone et al. (1981). Samples for spectrophotometric measurements were prepared by diluting concentrated hemoglobin stock solutions into a 65% v/v glycerol-buffer mixture (0.1 M phosphate buffer pH 7.0 in water at room temperature) to give a final concentration of about 10 μM in heme. The HbI solutions were equilibrated under a nitrogen atmosphere in a tonometer; thereafter, a small amount of dithionite (to give a final concentration $\approx 3 \cdot 10^{-4}$ M) was added. For measurements on the deoxy derivative, the hemoglobin solutions were transferred anaerobically from the tonometer to the cuvette (1 cm pathlength, methacrylate, Kartell) and to the optical dewar. Samples of HbI-CO and HbI-NO were prepared by equilibrating the hemoglobin solution in the tonometer with 1 atm of the respective gas. Spectra (500–380 nm) were measured on a Jasco Uvidec 650 spectrophotometer (Easton, MD) with a 0.4 nm bandwidth, 1 s time constant, 40 nm/min scan speed. The baseline (cuvette + solvent) was measured at room temperature and subtracted from each spectrum. In fact, in the spectral range of interest, the baseline does not depend on temperature and the absorption, because of the

Received for publication 31 January 1994 and in final form 6 July 1994.

Address reprint requests to Dr. Alberto Boffi, CNR Center of Molecular Biology c/o Dept. of Biochemical Sciences, University of "La Sapienza," 00185 Roma, Italy. Tel.: 39-6-494-0543; Fax: 39-6-444-0062.

0006-3495/94/10/1713/11 $2.00

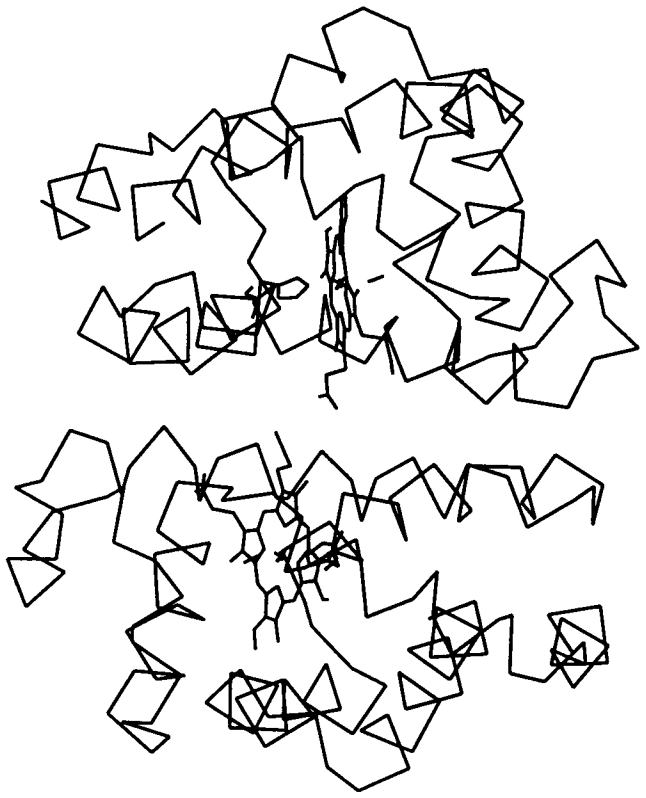

FIGURE 1 Diagram of *S. inaequivalvis* carbonmonoxy HbI. In addition to the α-carbon plot and the two heme groups, the side chains for the proximal His-101 and the bound CO molecules are shown. (Taken from the 2.4 Å resolution structure, Protein Data Bank, Brookhaven National Laboratory).

low dithionite concentrations used, becomes relevant only at wavelengths lower than ≈370 nm.

For flash photolysis measurements, the protein stock solution was diluted with a phosphate buffer-glycerol mixture. Final concentrations were ≈65 μM heme in 0.1 M phosphate buffer, pH 7.0 (in water at room temperature) and 75% v/v glycerol. Immediately after preparation, the sample was transferred anaerobically into a gold-plated copper cell (1.3 mm pathlength) that was mounted in a CF1204 cryostat equipped with a ITC-4 temperature controller (Oxford Instruments Ltd., Osney Mead, Oxford, OX2 0DX, UK). CO rebinding after photolysis was monitored in the 400–500 nm region using the instrumentation described elsewhere (Di Iorio et al., 1991). Between 5 and 10 traces were recorded for each temperature and/or wavelength. The data were then averaged to yield between 15 and 40 points per curve. For measurements between 15 and 130 K, after each flash the sample was heated to 140 K, to ensure complete rebinding and relaxation. The energy of the photolyzing pulse was high enough to ensure complete photolysis at all temperatures.

HbI concentrations were determined spectrophotometrically in the CO form on the basis of an extinction coefficient of 178 $mM^{-1}\,cm^{-1}$ at 421 nm (Chiancone et al., 1981). Absorption spectra were recorded on a Cary 219 (Varian Associates Inc., Palo Alto, CA) or on a photodiode array spectrophotometer HP-8452A (Hewlett Packard, San Diego, CA).

Data analysis

Optical spectra

In this paper, the analysis of the Soret band profile as a function of temperature has been carried out according to Di Pace et al. (1992) and to Cupane et al. (1993a). Only the principal aspects of the analysis will be given here.

The Soret band profiles are described as the convolution of three terms:

$$A(\nu) = L(\nu) \otimes G(\nu) \otimes P(\nu). \tag{1}$$

The first term, $L(\nu)$, is the usual Lorentzian lineshape for an absorption band; it can be expressed as

$$L(\nu) = M\nu \sum_{m_1,\ldots,m_{N_h}}^{\infty} \left[\prod_i^{N_h} \frac{S_i^{m_i} e^{-S_i}}{m_i!} \right] \times \frac{\Gamma}{[\nu - \nu' - \sum_i^{N_h} m_i R_i \nu_i]^2 + \Gamma^2}, \tag{2}$$

where M is a constant proportional to the square of the electric dipole moment operator; Γ is a damping factor related to the finite lifetime of the excited state; the product extends to all the N_h high frequency heme vibrational modes ($h\nu_i > K_B T$) coupled to the electronic transition and the summations to their occupation numbers; the coupling of the electronic transition with high frequency modes is expressed in terms of linear, S_i, and quadratic, R_i, coupling constants. In Eq. 1, therefore, the term $L(\nu)$ takes into account the natural (homogeneous) width of the electronic transition together with its coupling with high frequency modes; according to Eq. 2, the spectrum results from the superposition of a series of Lorentzians (one series for each high frequency mode) whose fundamental transition is centered at ν': within each series, the Lorentzians are spaced by multiples of the frequency of the vibrational mode, ν_i.

The coupling of the electronic transition with a "bath" of low frequency modes (arising from both the heme and protein) introduces the second term, $G(\nu)$, in Eq. 1; it is treated within the so-called "short times approximation" (Chan and Page, 1983) and gives rise to a Gaussian distribution of ν' values:

$$G(\nu) = \frac{1}{\sqrt{2\pi}\sigma(T)} \exp\left(- \frac{[\nu' - \nu_0(T)]^2}{2\sigma^2(T)} \right). \tag{3}$$

When the effects of coupling with both high and low frequency modes are taken into account, the spectral lineshape is given by a superposition of Voigtians (convolution of a Lorentzian with a Gaussian):

$$V(\nu) = M\nu \sum_{m_1,\ldots,m_{N_h}}^{\infty} \left[\prod_i^{N_h} \frac{S_i^{m_i} e^{-S_i}}{m_i!} \right] \int d\nu' \frac{\Gamma}{[\nu - \nu' - \sum_i^{N_h} m_i R_i \nu_i]^2 + \Gamma^2} \times \frac{\exp\{-[\nu' - \nu_0(T)]^2 / 2\sigma^2(T)\}}{\sqrt{2\pi}\sigma(T)}. \tag{4}$$

Parameters $\sigma(T)$ and $\nu_0(T)$ in Eqs. 3 and 4 depend upon temperature. Within the harmonic approximation, this dependence is expressed as

$$\sigma^2(T) = NSR^2\langle\nu\rangle^2 \coth(h\langle\nu\rangle / 2K_B T) \tag{5}$$

$$\nu_0(T) = \nu_{00} - \tfrac{1}{4} N\langle\nu\rangle (1 - R) \coth(h\langle\nu\rangle / 2K_B T) + C, \tag{6}$$

where $\langle\nu\rangle$, S, and R are the mean effective frequency, linear, and quadratic coupling constants, respectively, of the low frequency bath, N is the number of soft modes, ν_{00} is the frequency of the purely electronic transition, and C takes other temperature-independent contributions to the peak position into account.[1]

Further contributions to the spectral linewidth can arise from conformational heterogeneity (inhomogeneous broadening) caused by the presence of conformational substates (Frauenfelder et al., 1988; Örmos et al., 1990) and different heme group environments. Inhomogeneous broadening can be taken into account by assuming a distribution of the ν_{00} frequency, which is independent of temperature. In the liganded derivatives, the metal is locked in the heme plane by the ligand molecule and, therefore, the conformational distribution of heme group environments (assumed to be

[1] Parameters S and R in Eqs. 5 and 6 depend upon $\langle\nu\rangle$; their expressions are $S = h\langle\nu\rangle\Delta^2/2$ and $R = \langle\nu_u\rangle^2/\langle\nu\rangle^2$, where $\langle\nu_u\rangle$ and Δ are the average frequency of the thermal "bath" and the effective displacement of nuclear equilibrium positions in the excited electronic configuration.

Gaussian) maps into a Gaussian distribution of spectral transition energies. Thus, for the CO and NO derivatives, the ν_{00} distribution is given by

$$P(\nu_{00}) = \frac{1}{\sqrt{2\pi}\sigma_{in}} \exp\left(-\frac{[\nu_{00} - \nu_{00}^*]^2}{2\sigma_{in}^2}\right). \quad (7)$$

The convolution with a further Gaussian term does not alter the overall shape or symmetry of the band but simply adds a constant term σ_{in}^2 to the temperature dependence of σ^2 that, for liganded derivatives, therefore becomes

$$\sigma^2(T) = NSR^2\langle\nu\rangle^2 \coth(h\langle\nu\rangle/2K_B\tau) + \sigma_{in}^2. \quad (8)$$

In the case of deoxy hemoproteins, in which the iron is out of the heme plane, the conformational heterogeneity contributes a non-Gaussian distribution of ν_{00} transition frequencies (Srajer et al., 1986; Srajer and Champion, 1991). An analytical expression for this distribution has been developed (Srajer et al., 1986) assuming that ν_{00} depends quadratically upon a generalized, statistically distributed, iron coordinate Q:

$$P(\nu_{00}) = \frac{\exp(\mathcal{A}) + \exp(\mathcal{B})}{2\delta\sqrt{2\pi b[\nu_{00} - \nu_{00}^*]}} \quad (9)$$

where

$$\mathcal{A} = -\frac{[\sqrt{\nu_{00} - \nu_{00}^*} + Q_0\sqrt{b}]^2}{2b\delta^2} \qquad \mathcal{B} = -\frac{[\sqrt{\nu_{00} - \nu_{00}^*} - Q_0\sqrt{b}]^2}{2b\delta^2}$$

where Q_0 is the mean iron coordinate position and δ is the width of the distribution. The parameter b accounts for the dependence of the $\pi \rightarrow \pi^*$ transition energy upon the iron coordinates and reflects the electronic properties of the iron-porphyrin system (for a deeper discussion, see Srajer and Champion, 1991; Cupane et al., 1993a). It should be pointed out that only the quantities $Q_0\sqrt{b}$ and $\delta\sqrt{b}$ (and not Q_0 and/or δ) can be obtained from the fitting procedure. Moreover, for deoxy hemeproteins the σ^2 temperature dependence is given by Eq. 5 (i.e., with $\sigma_{in}^2 = 0$), because the effect of inhomogeneous broadening is considered explicitly in the parameter $\delta\sqrt{b}$.

The final expression apt to fit the spectra measured at various temperatures is given by the convolution of the Voigtians in Eq. 4 with the distribution $P(\nu_{00})$, i.e.,

$$A(\nu) = \int V(\nu) \times P(\nu_{00})\, d\nu_{00}, \quad (10)$$

where $V(\nu)$ is given by Eq. 4 and $P(\nu_{00})$ by Eqs. 7 and 9 for the liganded (CO and NO) and the deoxy derivatives, respectively.

Gaussian curves centered at 29,000 cm^{-1} (CO derivative), 28,000 cm^{-1} (NO derivative) and 26,500 cm^{-1} (deoxy derivative) were added, to take into account contributions from the N band (Di Pace et al., 1992; Cupane et al., 1993a). Fitting parameters were M, Γ, S_i, σ, ν_0, $Q_0 b$, and δb. The last two parameters were used for the fitting of the deoxy derivative only. The ν_i values of the high frequency modes were taken from resonance Raman spectra (Bangcharoenpaurpong et al., 1984; Spiro, 1983; Morikis et al., 1991; Song et al., 1993a). Because the less coupled modes do not contribute significantly to the observed spectra, only the most coupled ones have been considered, namely:

- for the deoxy derivative: $\nu = 370\ cm^{-1}$, $\nu = 674\ cm^{-1}$, $\nu = 1357\ cm^{-1}$;
- for the liganded derivatives: $\nu = 350\ cm^{-1}$, $\nu = 676\ cm^{-1}$, $\nu = 1100\ cm^{-1}$, $\nu = 1374\ cm^{-1}$.

The modes at 370 and 350 cm^{-1} in the deoxy and liganded derivatives, respectively, are average frequencies accounting for spectral regions characterized by several quasi-degenerate peaks. Equal ν values have been used for HbI, HbA, and SwMb; in fact, it has been shown by resonance Raman spectroscopy (Song et al., 1993a) that for the modes considered any frequency differences are less than 5 cm^{-1}, i.e., undetectable with optical spectroscopy.

CO rebinding kinetics after flash photolysis

The experimental time courses of CO rebinding were fitted with a sum of two kinetic components, each characterized by a discrete pre-exponential and distributed activation enthalpy. The use of two components was rendered necessary by the biphasic recombination kinetics. Accordingly, the reduced χ^2 values decreased by a factor of more than 20 with respect to the data fitting in terms of only one kinetic component. Therefore, the fraction of molecules that have not yet rebound a ligand molecule at time t after photolysis is given by

$$N(t) = f_1 \int dH\, g_1(H)\exp[-k0_1\exp(-H/RT)t] + f_2 \int dH\, g_2(H)\exp[-k0_2\exp(-H/RT)t], \quad (11)$$

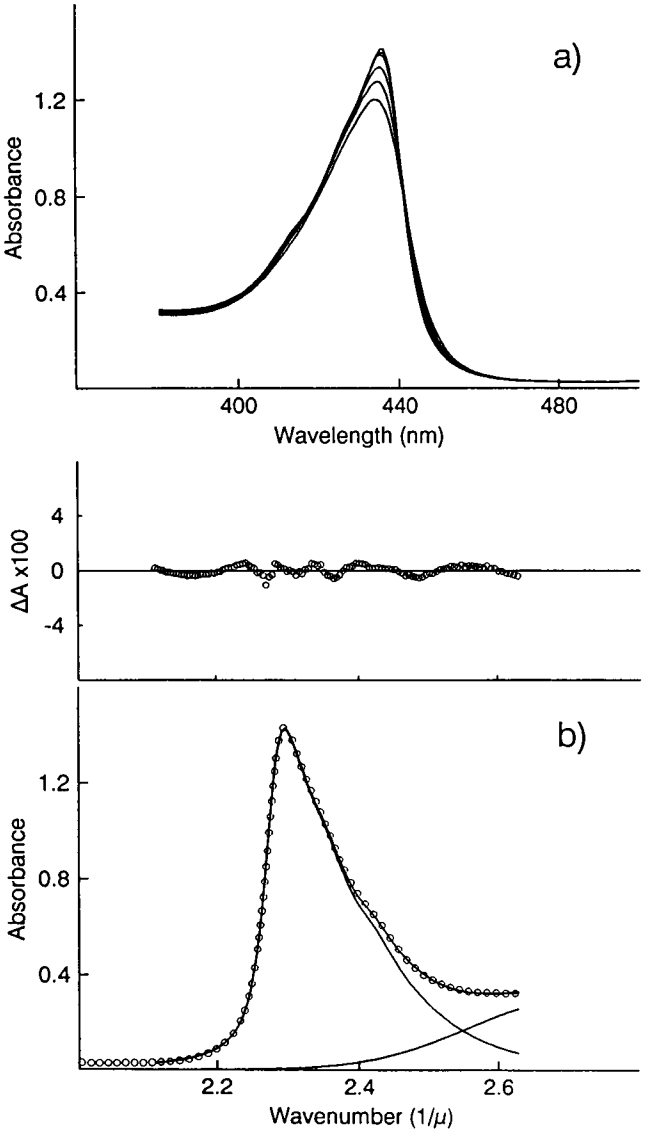

FIGURE 2 (*a*) Absorption spectra of the deoxy HbI at various temperatures in the range 300–10 K; (*b*) Deconvolution of deoxy HbI spectrum at 10 K in terms of Eq. 3. Circles are the experimental points; continuous lines represent the Soret band fitted in terms of Eq. 3, the contributions from the N band and the overall synthesized band profile. For clarity, not all of the experimental points are included. The residuals are also reported in the upper part of panel *b* on an expanded scale.

TABLE 1 Low temperature (T = 10 K) linear coupling constants of the high frequency modes and Γ values for the proteins investigated

	S_{370}	S_{674}	S_{1100}	S_{1357}	Γ/cm^{-1}
HbI	0.05 ± 0.01	0.08 ± 0.01	<0.01	0.06 ± 0.01	180 ± 5
HbA‡	0.11 ± 0.02	0.21 ± 0.02	<0.01	0.05 ± 0.01	175 ± 9
SwMb‡	0.32 ± 0.02	0.24 ± 0.02	<0.01	0.10 ± 0.01	180 ± 10
	S_{350}	S_{676}	S_{1100}	S_{1374}	Γ/cm^{-1}
HbI-NO	<0.01*	0.13 ± 0.01	<0.01	0.11 ± 0.02	403 ± 5
HcI-CO	<0.01	0.08 ± 0.01	<0.01	0.09 ± 0.01	250 ± 5
HbA-CO§	0.05 ± 0.01	0.07 ± 0.01	0.02 ± 0.01	0.08 ± 0.01	215 ± 4
SwMb-CO§	0.12 ± 0.02	0.06 ± 0.01	0.02 ± 0.01	0.09 ± 0.01	211 ± 7

* S_{350} cannot be estimated for the NO derivative, because of the large Γ value.
‡ Data from Cupane et al. (1993a).
§ Data from Di Pace et al. (1992).

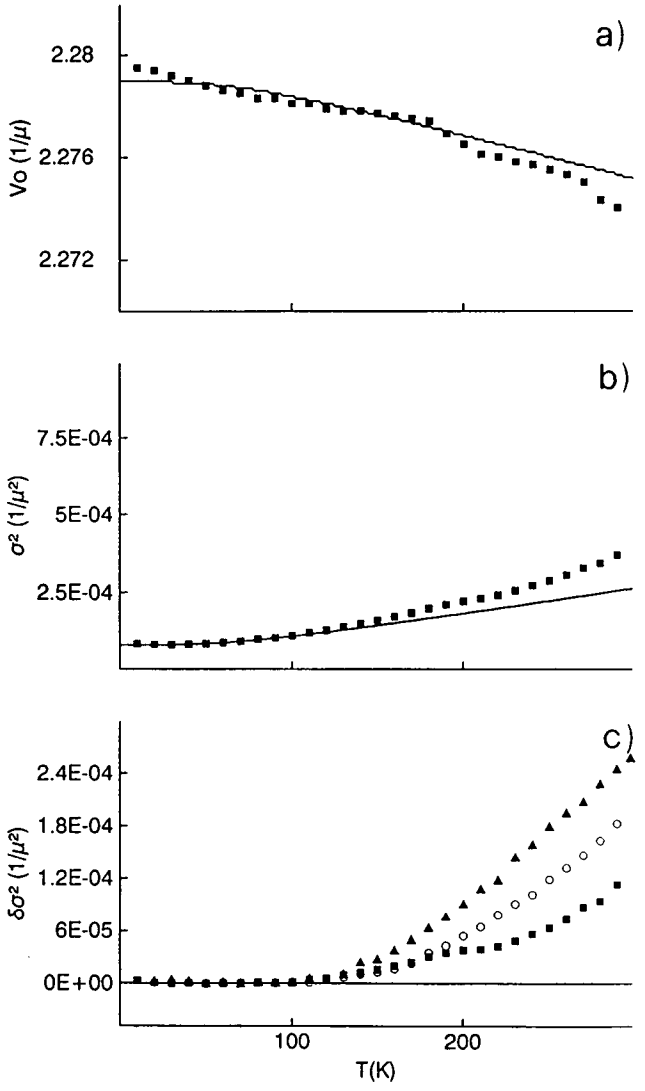

FIGURE 3 Temperature dependence of ν_0 (*a*) and σ^2 (*b*) values for the deoxy HbI (■). The continuous lines represent fittings of the data in the temperature range 10–110 K in terms of Eqs. 4 and 5; (*c*) $\Delta\sigma^2$ values for the deoxy HbI (■, present work), deoxy human HbA (*circles* from Cupane et al., 1993), and deoxy SwMb (*filled triangles* from Cupane et al., 1993).

with the boundary condition $f_1 + f_2 = 1$ and where R is the gas constant and T the absolute temperature. The enthalpy distribution $g(H)$, which describes the probability of finding the protein in a conformational substate characterized by an activation enthalpy between H and $H + dH$, is parametrized using the modified Γ function (Young and Bowne, 1984):

$$g_i(H) = H^{H_{peak_i}\cdot\Psi_i}\exp(-\Psi_i \cdot H), \quad (12)$$

in which H_{peak} is the peak position of the distribution and Ψ is a parameter related to the width of the distribution. Thus, in addition to the total amplitude of the absorbance change involved in the reaction, the fitting parameters are the relative amplitudes f_i, the pre-exponentials $k0_i$, the peak positions H_{peak_i} and Ψ_i. Fittings were performed by a global least-squares procedure, using the Marquardt algorithm (Marquardt, 1963). The integral involved in the distributed processes was computed numerically by the Romberg method to an accuracy of 10^{-5} OD units. Up to nine traces, recorded either at different wavelengths or at different temperatures, were fitted simultaneously in the OD space, weighing each point on the basis of its reciprocal variance. Convergence was considered to be reached when the reduced χ^2 change between two successive iterations was smaller than 10^{-4}. The error analysis on the individual parameters was done as described elsewhere (Di Iorio et al., 1991) and served also the purpose of avoiding local minima in the χ^2 hypersurface.

TABLE 2 Values of the parameters obtained by fitting the low temperature σ^2 behavior in terms of Eq. 2.

	NS*	⟨ν⟩/cm^{-1}	σ_{in}/cm^{-1}§
HbI	0.6 ± 0.1	120 ± 10	/
HbA‡	0.6 ± 0.1¶	140 ± 10¶	/
SwMb‡	0.7 ± 0.1¶	110 ± 10¶	/
HbI-NO	0.8 ± 0.2	225 ± 10	0 ± 20
HbI-CO	0.5 ± 0.1	208 ± 5	0 ± 20
HbA-CO‖	0.5 ± 0.2	170 ± 20	70 ± 23
SwMb-CO‖	0.3 ± 0.2	180 ± 30	53 ± 38

* NS values were obtained under the assumption $R^2 \approx 1$.
‡ Data from Cupane et al. (1993a).
§ For the deoxy derivatives, inhomogeneous broadening is taken into account by the parameter $\delta\sqrt{b}$.
¶ *NS* and ⟨ν⟩ values relative to SwMb reported in this work are slightly different from the analogous ones (NS = 0.7 and ⟨ν⟩ = 110) reported previously (Cupane et al., 1993a). This is because, to avoid the systematic misfits observed for deoxyhemoglobin and myoglobin at temperatures around 100 K and clearly evident in Fig. 4 of the paper by Cupane et al., 1993a, fittings of the σ^2 thermal behavior have been restricted, for the deoxy derivatives, to the temperature range 20–110 K.
‖ Data from Di Pace et al. (1992).

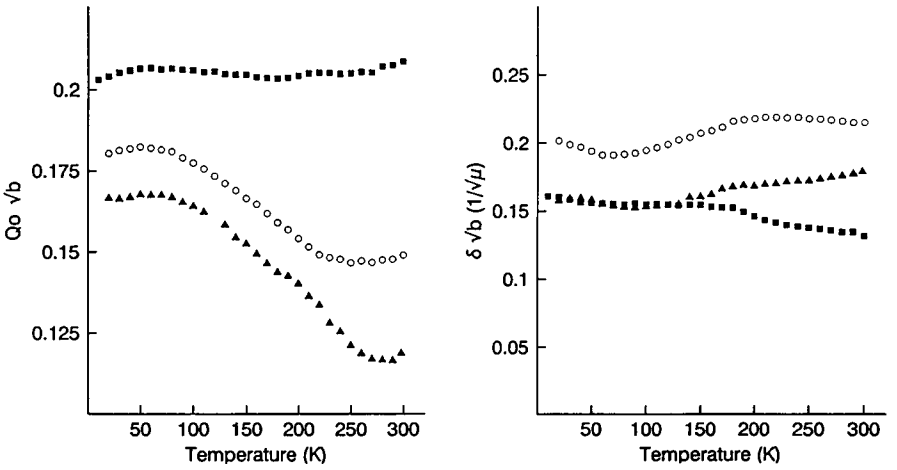

FIGURE 4 Temperature dependence of $Q_0\sqrt{b}$ (*left*) and of $\delta\sqrt{b}$ (*right*). Squares refer to Scapharca HbI (present work), and triangles and open circles refer to to SwMb and human HbA, respectively (Cupane et al., 1993). Error bars at high temperature are less than 2%; at low temperature, the errors decrease by more than a factor of two.

RESULTS

Optical spectra

Fig. 2 *a* shows the spectra of deoxy HbI at various temperatures between 300 and 10 K. A fit of the 10 K spectrum in terms of Eq. 10 is shown in Fig. 2 *b* together with the residuals on an expanded scale. The coupling constants and Γ values obtained from the fittings are listed in Table 1, in comparison with those obtained for human hemoglobin (HbA) and for Sperm whale myoglobin (SwMb).

The temperature dependence of the peak frequency (ν_0) and of the Gaussian width (σ^2) is reported in Fig. 3, *a* and *b*, respectively. Both parameters follow the behavior predicted by the harmonic approximation (Eqs. 5 and 6) only over a limited temperature range. This is particularly evident for σ^2 because a straight line tangent to the high temperature experimental data would extrapolate at $T = 0$ to negative values. A proper fit in terms of Eqs. 5 and 6 can be performed only in the range 10–110 K; the continuous lines in Fig. 3, *a* and *b* represent such fittings with the parameter values reported in Table 2, where analogous data relative to HbA and Sw-Mb are included for comparison.

The deviations of σ^2 values from the harmonic behavior observed at temperatures higher than ≈120 K are similar to those already reported for other hemeproteins and are attributed to the onset of nonharmonic nuclear motions. These nonharmonic contributions ($\Delta\sigma^2$, i.e., the difference between the experimental σ^2 values and the continuous lines in Fig. 3 *b*) are reported in Fig. 3 *c* and compared with the analogous quantities relative to HbA and Sw-Mb.

Concerning the temperature dependence of parameter ν_0, deviations from the harmonic behavior are difficult to analyze, because they can arise from the above-mentioned nonharmonic contributions to nuclear motions, from a temperature dependence of the term ν_{00} in Eq. 6 (see, e.g., Cordone et al., 1988; Di Iorio et al., 1991; Di Pace et al., 1992) or from both effects.

The other two parameters necessary to take into account the inhomogeneous broadening of the deoxy spectra ($Q_0\sqrt{b}$ and $\delta\sqrt{b}$; see Data Analysis) are reported in Fig. 4. It can be seen that, within 10%, these parameters do not

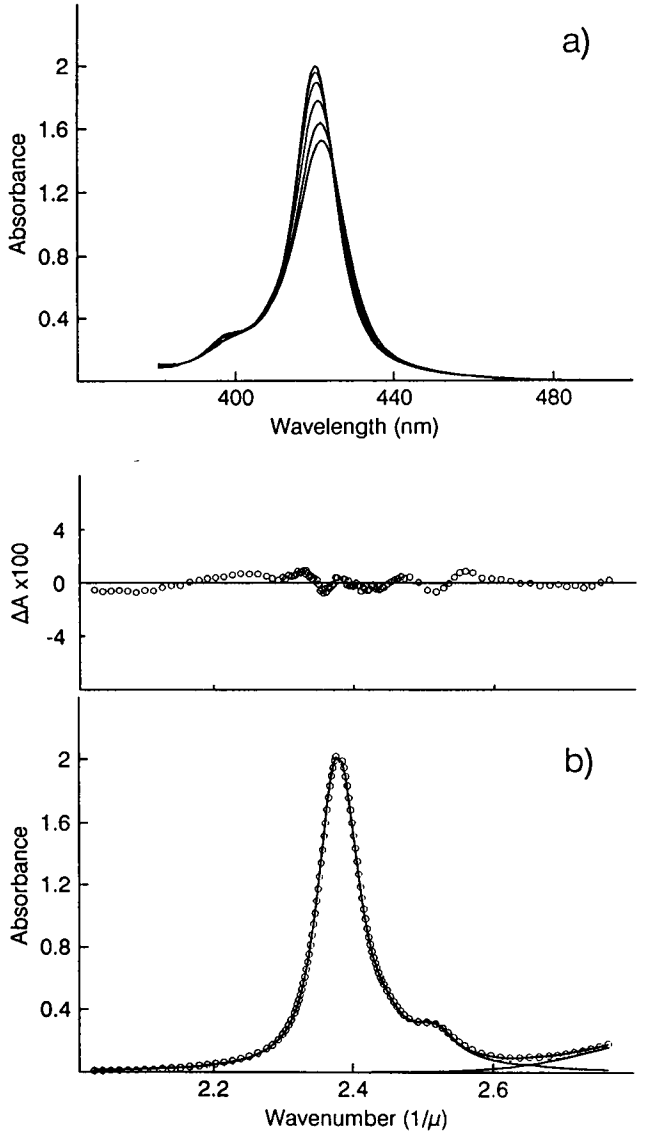

FIGURE 5 (*a*) Absorption spectra of carbonmonoxy derivative of HbI at various temperatures in the range 300–10 K; (*b*) Deconvolution of HbI-CO spectrum at 10 K in terms of Eq. 1. Symbols are as in Fig. 1. For clarity, not all of the experimental points are included. The residuals are also reported in the upper part of panel *b* on an expanded scale.

depend upon temperature. The ≈25% decrease of $Q_0\sqrt{b}$ observed for HbA and for SwMb when temperature increases from 20 to 300 K (Cupane et al., 1993a; see Fig. 4) is not observed for HbI.

The spectra of HbI-CO and HbI-NO measured at various temperatures between 10 and 300 K are shown in Figs. 5 *a* and 6 *a*, respectively. The spectra have been fitted by use of Eq. 10 as described in Data analysis. Figs. 5 *b* and 6 *b* show the fit to the spectra at 10 K, together with the residuals on an expanded scale. The values of the linear coupling constants S_i and of the damping factor Γ obtained from the fitting procedure are listed in Table 1 together with the same parameters obtained for the CO derivatives of SW-Mb and HbA (Di Pace et al., 1992). The temperature dependence of ν_0 and σ^2 are reported in Fig. 7, *a* and *b*, respectively.

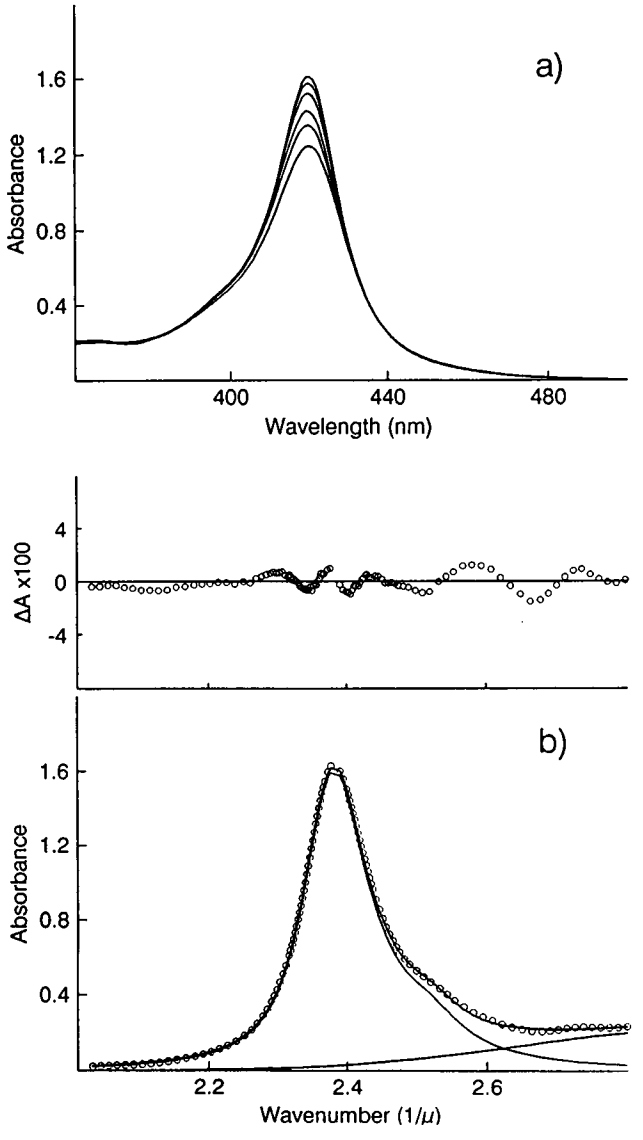

FIGURE 6 (*a*) Absorption spectra of nitrosyl derivative of HbI at various temperatures in the range 300–10 K; (*b*) Deconvolution of HbI-NO spectrum at 10 K in terms of Eq. 1. Symbols are as in Fig. 1. For clarity, not all of the experimental points are included. The residuals are also reported in the upper part of panel *b* on an expanded scale.

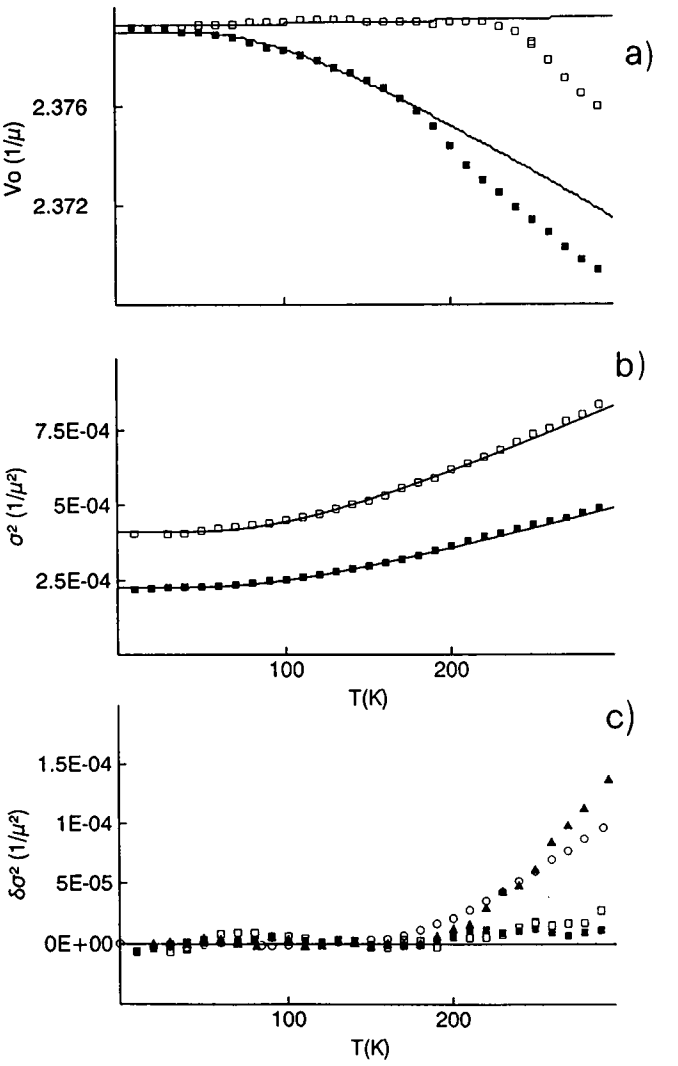

FIGURE 7 Temperature dependence of ν_0 (*a*) and σ^2 (*b*) values for HbI-CO (■) and HbI-NO (□). The continuous lines represent fittings of the data in the temperature range 10–160 K in terms of Eqs. 4 and 5. (*c*) $\Delta\sigma^2$ values for HbI-CO (■, present work), HbI-NO (□, present work), human HbA-CO and SwMb-CO (*circles* and *filled triangles*, respectively, data from Di Pace et al., 1992).

At variance from the deoxy derivative, for both liganded HbI derivatives, the σ^2 temperature dependence follows the prediction of the harmonic approximation (Eq. 8; solid lines in Fig. 7 *b*), and nonharmonic contributions are, if any, very small. This is shown in Fig. 7 *c*, where δ/σ^2 values obtained for HbI-CO and HbI-NO are reported together with analogous data relative to HbA-CO and Sw-Mb-CO. The deviations from the behavior predicted by Eq. 6 observed for ν_0 at temperatures higher than ~200 K (Fig. 7 *a*) are therefore attributed to variations in the parameter ν_{00} of Eq. 6 occurring at these temperatures. Parameter values resulting from the fittings of σ^2 values relative to liganded HbI derivatives with Eq. 8 are reported in Table 2, in comparison with analogous values relative to HbA-CO and Sw-Mb-CO.

CO rebinding kinetics

Fig. 8 depicts the kinetics of CO rebinding to HbI after photolysis over the temperature range 60–180 K. The fitting parameters are listed in Table 3. Up to ≈200 K, ligand recombination is assumed to occur only within the heme pocket (Austin et al., 1975). The two kinetic components needed to account for the biphasic time courses of CO rebinding differ in peak position (H_{peak}) and width of the enthalpy distributions, but have the same preexponential factors; moreover, H_{peak} and width of the two enthalpy distributions do not depend on temperature up to the solvent glass transition (≈180 K). At higher temperatures, the width of the two distributions starts to increase. Fig. 9 shows the temperature dependence of the fractional amplitudes (f_i) of the two kinetic processes. The f_i values depend upon temperature; in particular, f_1 decreases whereas f_2 increases with increase in temperature.

At temperatures higher than 200 K, no reasonable fitting of the data could be obtained unless at least four processes with temperature-dependent parameters were assumed to take place simultaneously. This type of analysis, however, did not lead to unique solutions and, therefore, is not reported. On the other hand, models that implicitly link the low and high temperature behavior through protein relaxation (e.g., Steinbach et al., 1991) fail to account for a complex kinetic behavior such as that of HbI, although they work well in the case of noncooperative systems. An analysis of the high temperature data, therefore, must await for models of more general applicability.

The "kinetic" difference spectrum for the total CO rebinding process has been obtained at 15 K over the wavelength range 400–450 nm from absorbance changes extrapolated to time 0 and is reported in Fig. 10, in comparison with the "static" deoxy − CO difference spectrum measured at 10 K. For the sake of clarity, the spectra of deoxy and CO-HbI at 10 K are also shown. Data analogous to those of Fig. 10, relative to SwMb, are reported in Fig. 11.

DISCUSSION

Analysis of spectral lineshapes

Information on the stereodynamic properties of the active site in HbI can already be obtained from the values of the coupling constants with high frequency modes (S_i) reported in Table 1. In fact, sizable differences between HbI on one side and HbA and SwMb on the other are observed for S_{676} (only for the deoxy derivatives) and for S_{350} (or S_{370}) for both deoxy and CO derivatives: for these modes, the S_i values relative to HbI are smaller than those relative to HbA and SwMb. In contrast, the S_i values relative to the modes at 1374 (or 1357) and 1100 cm^{-1} are very similar for the three proteins. These findings are in line with recent resonance Raman spectroscopy data (Song et al., 1993a) that showed that the spectra of HbI and HbA differ in the lower frequency region (200–800 cm^{-1}), but not in the higher frequency region (800–1700 cm^{-1}). The latter result has been taken as evidence for different interactions between the heme and the amino acid residues in the pocket of HbI with respect to HbA, because the lower frequency modes are sensitive to the conformation of the peripheral substituents of the heme (Spiro, 1983; Rousseau et al., 1993). The optical spectroscopy data reported in Table 1 confirm this interpretation.

The electronic transition responsible for the Soret band of HbI is coupled with a bath of low frequency nuclear motions, as in previously studied hemeproteins. In the deoxy derivative, the average frequency and coupling constants of the bath are very similar to those of HbA and SwMb (Table 2), whereas the nonharmonic contributions to nuclear motions

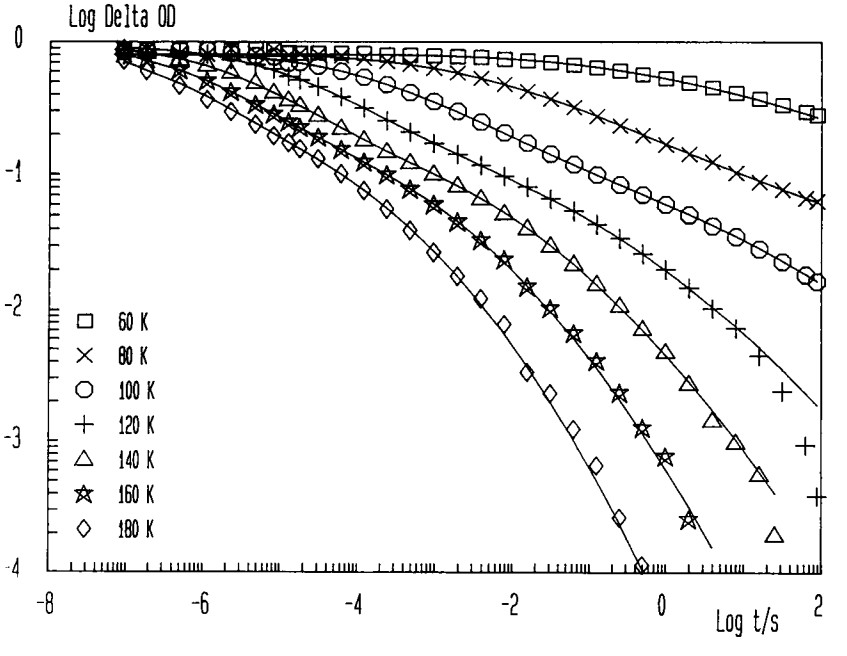

FIGURE 8 Time courses of CO rebinding to HbI after photolysis. Temperature range: 40–110 K (*A*), 120–200 K. Continuous lines represent the fitted curves corresponding to the parameters given in Table 3.

TABLE 3 Values of the fitting parameters for the two processes used to analyze the CO rebinding kinetics to HbI between 60 and 200 K.

T (K)	f_1	H_{peak1}	$FWHM_1$	ψ_1	Log kO_1	f_2	H_{peak1}	$FWHM_2$	ψ_2	Log kO_2
60	0.884	11.53	5.90	1.97	9.51	0.116	18.69	7.50	1.87	9.51
80	0.911	11.53	5.90	1.97	9.51	0.089	18.69	7.50	1.87	9.51
100	0.883	11.53	5.90	1.97	9.51	0.117	18.69	7.50	1.87	9.51
120	0.866	11.53	5.90	1.97	9.51	0.134	18.69	7.50	1.87	9.51
140	0.842	11.53	5.90	1.97	9.51	0.158	18.69	7.50	1.87	9.51
160	0.804	11.53	5.90	1.97	9.51	0.196	18.69	7.50	1.87	9.51
180	0.772	11.53	5.90	1.97	9.51	0.228	18.69	7.50	1.87	9.51
190	0.724	11.53		1.63	9.51	0.276	18.69		1.59	9.51
200	0.686	11.53		0.96	9.51	0.314	18.69		1.09	9.51

The full width at half maximum (FWHM) is not a fitting parameter and is computed from the $g(H)$ distribution as defined by H_{peak} and ψ (Eq. 7). The 67% confidence limits of the data reported are ~10%.

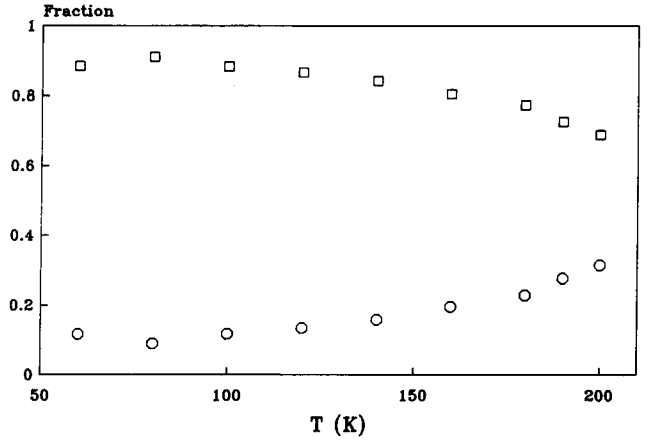

FIGURE 9 Temperature dependence of the fractional amplitudes of the kinetic components needed to account for the flash photolysis data. Fractions f_1 and f_2 correspond to processes having the lower and the higher H_{peak}, respectively.

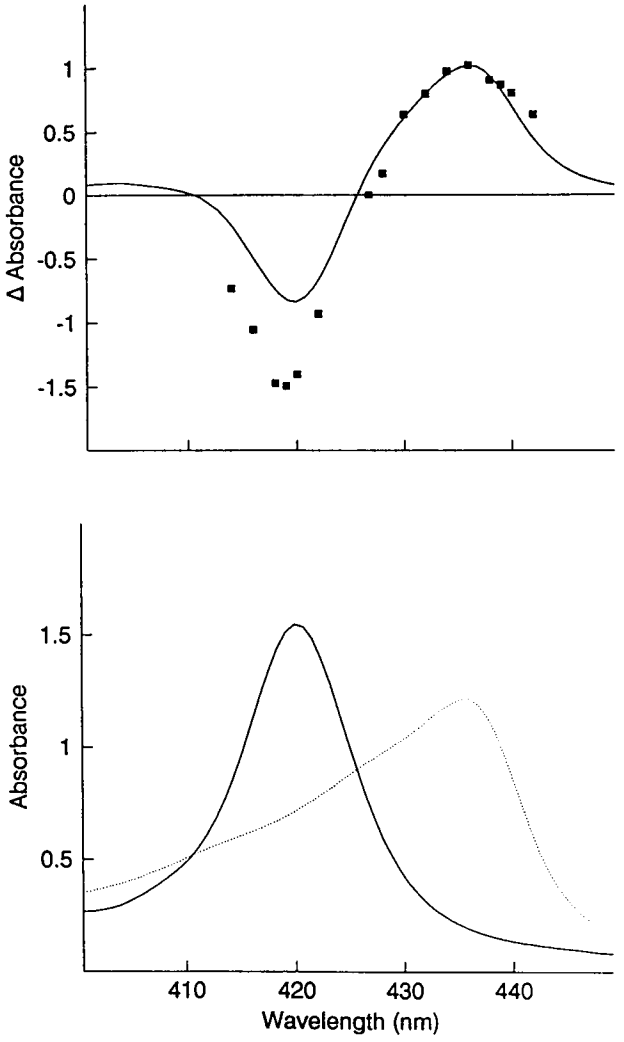

FIGURE 10 (*top*) Squares represent the "kinetic" difference spectrum (photoproduct minus HbI-CO) at 15 K; the continuous line represents the "static" difference spectrum (HbI minus HbI-CO) at 10 K. Spectral data have been suitably normalized before subtraction and the wavelength calibration of the optical apparata in Zürich and in Palermo have been carefully checked. (*bottom*) "Static" spectra of HbI (·····) and of HbI-CO (——) at 10 K.

are significantly smaller (Fig. 3 *c*). On this basis, the structure of the heme environment appears to be more rigid in deoxy HbI than in deoxy-HbA or -SwMb. In addition, deoxy HbI is characterized by a reduced mobility of the iron atom with respect to the heme plane as a function of temperature; thus, the value of parameter $Q_0\sqrt{b}$ is constant with increase in temperature, whereas it decreases in all the other hemeproteins studied (Cupane et al., 1993a). Both properties can be ascribed to the involvement of the heme-carrying E and F helices in the intersubunit contact and, more specifically, to the unique network of interactions that the heme propionates establish with the F helix of the contralateral subunit. However, contributions from residues on the distal and/or proximal side of the heme pocket cannot be excluded.

The liganded derivatives of HbI display an even more unusual temperature dependence of the Soret spectra. In fact, the σ^2 temperature dependence conforms to the prediction of the harmonic approximation over the whole temperature range analyzed (Fig. 7, *b* and *c*). This behavior is in marked contrast with that of all other hemoglobins and myoglobins investigated, in which significant nonharmonic contributions are evident above ≈180 K (Di Pace et al., 1992).

The data in Table 2 show that the HbI liganded derivatives are characterized by a larger value of the average frequency and linear coupling constants of the low frequency bath and by much smaller σ_{in} values relative to HbA-CO and SwMb-CO. All these features consistently point out an unusual

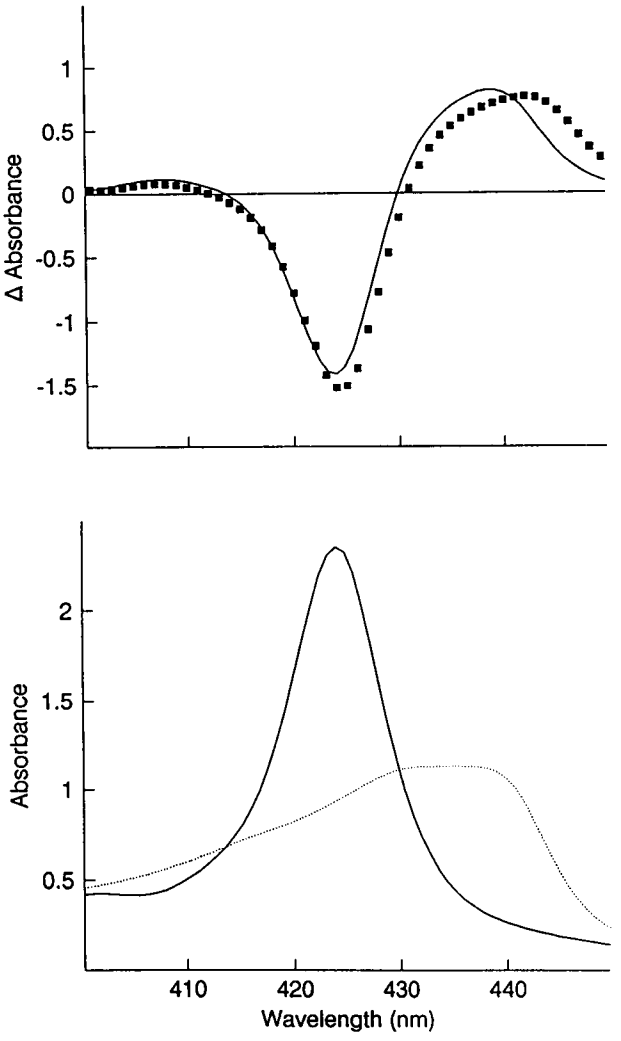

FIGURE 11 Data analogous to those reported in Fig. 10, relative to Sw-Mb. (*top*) The photoproduct-SwMbCO difference spectrum (■) is courtesy of Dr. Pal Örmos and has been measured at 10 K with a Cary-Olis spectrophotometer; continuous line represents the "static" difference spectrum (Sw-Mb minus Sw-Mb-CO) at 10 K. (*bottom*) "Static" spectra of Sw-Mb (·····) and Sw-Mb-CO (——) at 10 K.

rigidity of the heme environment in HbI that is particularly enhanced in the liganded derivatives. The stabilizing effect of the ligand on the dynamics of the heme pocket is present in all heme proteins studied (compare Figs. 3 *c* and 7 *c*; see also Cupane et al., 1993a). This effect is more pronounced in the case of HbI and is likely to be caused by interactions of the bound ligand with the distal heme pocket. In fact, recent resonance Raman measurements (Song et al., 1993a) show that in HbI-CO the bound ligand is significantly tilted off axis because of distal site crowding; the movements of the bound ligand within the heme pocket should therefore be extremely reduced. The data in Table 2 also show that for HbI-CO σ_{in} is much smaller than for HbA-CO or SwMb-CO, thus indicating a much smaller degree of conformational heterogeneity in HbI with respect to the other two proteins. Consistently, FTIR spectroscopy has shown that the IR absorption lines of both the CO-bound and the photodissociated derivatives (the so called A and B states; Ansari et al., 1987) are narrower for HbI than for HbA (Song et al., 1993b).

It is of interest that the temperature dependence of the line-broadening parameter σ^2 is very similar in the CO and NO derivatives, despite the different binding geometry of the two ligands. On this basis, the study of the NO derivatives of other hemeproteins should provide information on the role of distal side interactions on protein fluctuations (Braunstein et al., 1988).

Analysis of the CO rebinding kinetics

The two processes that describe the low temperature kinetics of CO rebinding to HbI have broad enthalpy distributions peaked at high enthalpy values if compared with SwMb and isolated human hemoglobin subunits. This finding, in agreement with the optical spectroscopy data, suggests a considerably more rigid structure in HbI than in the other hemeproteins studied to date (Di Iorio et al., 1991). The features of the two distributions (H_{peak} and width) are temperature-independent up to the glass transition temperature (Table 3). An analysis of the kinetic traces at higher temperatures (above 200 K) is not reported because the fitting procedure does not lead to a unique solution because of the complexity of the situation.

The biphasic kinetics observed at low temperatures could in principle be related to the formation of slowly rebinding states because of structural relaxation after photolysis of the ligand. However, the temperature independence of the fractions of the two kinetic components (Table 3) renders this hypothesis unlikely. It may be envisaged that the presence of two geminate processes in the CO rebinding kinetics to HbI depends on the coexistence of two heme pocket conformations roughly corresponding to the pocket geometry of the deoxy and CO derivatives detected by x-ray analysis (Royer et al., 1989, 1990). Thus, ligand recombination occurs mostly (f_1) within a "CO-like" pocket characterized by the lower peak activation enthalpy of CO rebinding (H_{peak}) and the narrower enthalpy distribution ($g(H)$). However, a small fraction of the proteins (f_2) has a "deoxy-like" heme-pocket configuration characterized by the higher H_{peak} value and the broader $g(H)$ distribution. The thermal evolution of the fractional amplitudes of the two processes (Fig. 9) is consistent with this interpretation. Below the glass transition temperature, a small change in the relative populations of the two states is observed, in line with a highly reduced rotational mobility of the amino-acid side chains (Loncharich and Brooks, 1990; Cupane et al., 1993b). At the glass transition temperature, photolysis starts to be accompanied by conversion of the CO to the deoxy configuration and, therefore, process 2 starts to relax and becomes more populated.

Based on FTIR measurements on the CO-photoproduct (Song et al., 1993b) that show that at 4.2 K a single conformational substate (the B_1 state) is populated, the enthalpic barrier associated with process 1 can be attributed to CO rebinding from the B_1 state. In turn, this assignment requires the B_1 state to be populated significantly at least up to 180

K. The fact that protein molecules responsible for process 2 are not seen by FTIR spectroscopy can be because either the two photolyzed conformers have similar CO stretching frequencies or because conformer 2 is little populated at low temperature (f_2 is less than 10% at 60 K, see Fig. 9). If this is the case, FTIR spectra of the CO-photoproduct measured at 150–200 K should exhibit heterogeneity.

At 10 K, the kinetic difference spectrum of the HBI photoproduct, i.e., the difference spectrum obtained by subtracting the CO spectrum from the "time 0" spectrum measured $\sim 10^{-8}$ s after photolysis, shows remarkable features when compared with the static deoxy-CO difference spectrum measured under comparable conditions (Fig. 10). The two spectra differ markedly in the blue side of the Soret region. The difference does not reflect only a spectral shift, but indicates that the Soret spectrum of the photoproduct is characterized by a smaller band asymmetry relative to the spectrum of deoxy hemoglobin. This finding can be ascribed to a lower value of parameter $Q_0\sqrt{b}$ in the term $P(\nu_{00})$ of Eq. 9. On this basis, in the "time 0" photoproduct of HbI at low temperature the iron atom appears to be almost in plane with respect to the heme group. For SwMb at 10 K the differences between static and kinetic difference spectra, although present, are not as marked as for HbI, particularly in the blue side of the Soret region (Fig. 11). It may be envisaged that in the 10 K SwMb photoproduct the iron atom is already out of the mean heme plane (although not in the normal deoxy position). Consistently, EXAFS data indicate that the Fe-mean heme plane distance is 0.4 Å in the 10 K SwMb photoproduct, as compared with 0.55 Å in the normal deoxy derivative (Powers et al., 1993).

In conclusion, the dynamic picture of HbI that emerges from the present study points to an unusual rigidity of the heme environment. Whether this feature is caused by specific characteristics of the proximal and/or distal side of the heme pocket or whether it is related to the interactions that link the heme propionates across the interface to the F helix of the opposite subunit remains an open question that will be addressed by site directed mutagenesis.

We wish to express our gratitude to Dr. Pal Örmos (Hungarian Academy of Sciences, Szeged, Hungary) for making available to us the 10 K "kinetic" difference spectrum relative to SwMb. We are also indebted to Mr. G. Lapis, Mr. A. Lehman and Mr. M. Quartararo for technical help.

This work has been supported by grants from the Italian "Ministero per l'Universita' e per la Ricerca Scientifica e Tecnologica" to the Palermo group and to E. Chiancone, and by the Swiss National Science Foundation grant 31.9432.88 and ETH special credit 03586/41–1080.5 to the Zürich group. General indirect support to the Palermo group from the Sicilian "Comitato Regionale Ricerca Nucleare e Struttura della Materia" is also gratefully acknowledged.

REFERENCES

Ansari, A., J. Berendzen, D. Braunstein, B. R. Cowen, H. Frauenfelder, M. K. Hong, I. E. T. Iben, J. B. Johnson, P. Ormos, T. B. Sauke, R. Scholl, A. Schulte, P. J. Steinbach, J. Vittitow, and R. D. Young. 1987. Rebinding and relaxation in the myoglobin pocket. *Biophys. Chem.* 26:337–355.

Austin, R. H., K. W. Beeson, L. Eisenstein, H. Frauenfelder, and I. C. Gunsalus. 1975. Dynamics of ligand binding to myoglobin. *Biochemistry.* 14:5355–5373.

Bangcharoenpaurpong, O., K. T. Schomacker, and P. M. Champion. 1984. A resonance Raman investigation of myoglobin and hemoglobin. *J. Am. Chem. Soc.* 106:5688–5698.

Braunstein, D., A. Ansari, J. Berendzen, B. R. Cowen, K. D. Egeberg, H. Frauenfelder, M. K. Hong, P. Ormos, T. B. Sauke, R. Scholl, A. Schulte, S. G. Sligar, B. A. Springer, P. J. Steinbach, and R. D. Young. 1988. Ligand binding to synthetic mutant myoglobin (His E7 → Gly): role of the distal histidine. *Proc. Natl. Acad. Sci. USA.* 85:8497–8501.

Chan, C. K., and J. B. Page. 1983. Temperature effects in the time correlator theory of resonance Raman scattering. *J. Chem. Phys.* 79: 5234–5250.

Chiancone, E., P. Vecchini, D. Verzili, F. Ascoli, and E. Antonini. 1981. Dimeric and tetrameric hemoglobins from the mollusc Scapharca inaequivalvis. *J. Mol. Biol.* 152:577–592.

Chiancone, E., D. Verzili, A. Boffi, W. E. Royer, Jr., and W. A. Hendrickson. 1990. A cooperative hemoglobin with directly communicating hemes. The Scapharca inaequivalvis homodimer. *Biophys. Chem.* 37:287–292.

Coletta, M., A. Boffi, P. Ascenzi, M. Brunori, and E. Chiancone. 1990. A novel mechanism of heme-heme interaction in the homodimeric hemoglobin of the clam Scapharca inaequivalvis. *J. Biol. Chem.* 265: 4828–4830.

Cordone, L., A. Cupane, M. Leone, E. Vitrano, and D. Bulone. 1988. Interaction between external medium and haem pocket in myoglobin probed by low-temperature optical spectroscopy. *J. Mol. Biol.* 198: 213–218.

Cupane, A., M. Leone, and E. Vitrano. 1993a. Protein dynamics: conformational disorder, vibrational coupling and anharmonicity in deoxyhemoglobin and myoglobin. *Eur. Biophys. J.* 21:385–391.

Cupane, A., M. Leone, E. Vitrano, L. Cordone, U. R. Hiltpold, K. H. Winterhalter, W. Yu, and E. E. Di Iorio. 1993b. Structure-dynamics-function relationships in Asian elephant (*Elephas maximus*) myoglobin. An optical spectroscopy and flash-photolysis study on functionally important motions. *Biophys. J.* 65:2461–2472.

Di Iorio, E. E. 1992. Protein dynamics. An overview on flash-photolysis over brod temperature ranges. *FEBS Lett.* 307:14–19.

Di Iorio, E. E., U. R. Hiltpold, D. Filipovic, K. H. Winterhalter, E. Gratton, E. Vitrano, A. Cupane, M. Leone, and L. Cordone. 1991. Protein dynamics: a comparative investigation on heme-proteins with different physiological roles. *Biophys. J.* 59:742–754.

Di Pace, A., A. Cupane, M. Leone, E. Vitrano, and L. Cordone. 1992. Vibrational coupling, spectral broadening mechanisms and anharmonicity effects in carbonmonoxy heme proteins studied by the temperature dependence of the Soret band lineshape. *Biophys. J.* 63:475–484.

Frauenfelder, H., F. Parak, and R. D. Young. 1988. Conformational substates in proteins. *Annu. Rev. Biophys. Biophys. Chem.* 17:451–479.

Loncharich, R. J., and B. R. Brooks. 1990. Temperature dependence of dynamics of hydrated myoglobin. *J. Mol. Biol.* 215:439–455.

Marquardt, D. W. 1963. An algorithm for least-squares estimation of non linear parameters. *J. Soc. Ind. Appl. Math.* 11:431–441.

Morikis, D., P. Li, O. Bangcharoenpaurpong, J. T. Sage, and P. M. Champion. 1991. Resonance Raman scattering as a probe of electron-nuclear coupling: applications to heme proteins. *J. Phys. Chem.* 95: 3391–3398.

Örmos, P., A. Ansari, D. Braunstein, B. R. Cowen, H. Frauenfelder, M. H. Hong, I. E. T. Iben, T. B. Sauke, P. Steinbach, and R. D. Young. 1990. Inhomogeneous broadening in spectral bands of carbonmonoxymyoglobin: the connection between spectral and functional heterogeneity. *Biophys. J.* 57:191–199.

Powers, L., R. Sinclair, S. Hallam, and I. Yamazaki. 1993. Hemeprotein catalysis: structure-function relationship. *Abstracts of the 11th International Biophysics Congress.* p. 90.

Rousseau, D. L., S. Song, J. M. Friedman, A. Boffi, and E. Chiancone. 1993. Heme-heme interaction in a homodimeric cooperative hemoglobin: evidence from transient Raman scattering. *J. Biol. Chem.* 264:5719–5723.

Royer, W. E., W. A. Hendrickson, and E. Chiancone. 1989. The 2.4 Å crystal structure of Scapharca dimeric hemoglobin. Cooperativity based on directly communicating hemes at a novel subunit interface. *J. Biol. Chem.* 264:21052–21061.

Royer, W. E., W. A. Hendrickson, and E. Chiancone. 1990. Structural transitions upon ligand binding in a cooperative dimeric hemoglobin. *Science.* 249:518–521.

Schomacker, K. T., and P. M. Champion. 1986. Investigations of spectral broadening mechanisms in biomolecules. *J. Chem. Phys.* 84:5314–5325.

Song, S., A. Boffi, E. Chiancone, and D. L. Rousseau. 1993a. Protein-heme interactions in hemoglobin from the mollusc Scapharca inaequivalvis. Evidence from resonance Raman scattering. *Biochemistry.* 32:6330–6336.

Song, S., L. Rothberg, D. L. Rousseau, A. Boffi, and E. Chiancone. 1993b. Metastable CO binding sites in the photoproduct of a novel cooperative dimeric hemoglobin. *Biophys. J.* 65:1959–1962.

Spiro, T. G. 1983. Iron Porphyrins. Vol. 2. A. B. P. Lever and H. B. Gray, editors. Addison Wesley Publishing Co., Reading, MA. 89–159.

Srajer, V., and P. M. Champion. 1991. Investigations of optical line shapes and kinetic hole burning in myoglobin. *Biochemistry.* 30:7390–7402.

Srajer, V., K. T. Schomacker, and P. M. Champion. 1986. Spectral broadening in biomolecules. *Phys. Rev. Lett.* 57:1267–1270.

Steinbach, P. J., A. Ansari, J. Berendzen, D. Braunstein, K. Chu, B. R. Cowen, D. Ehrenstein, H. Frauenfelder, J. B. Johnson, D. C. Lamb, S. Luck, J. R. Mourant, G. U. Nienhaus, P. Ormos, R. Philipp, A. Xie, and R. D. Young. 1991. Ligand binding to heme proteins: connection between dynamics and function. *Biochemistry.* 30:3988–4001.

Young, R. D., and S. F. Bowne. 1984. Conformational substates and barrier height distributions in ligand binding to heme proteins. *J. Chem. Phys.* 81:3730–3737.